



This is a repository copy of *More than just summed neuronal activity : how multiple cell types shape the BOLD response.*

White Rose Research Online URL for this paper:
<http://eprints.whiterose.ac.uk/166097/>

Version: Accepted Version

Article:

Howarth, C., Mishra, A. and Hall, C. (2020) More than just summed neuronal activity : how multiple cell types shape the BOLD response. *Philosophical Transactions of the Royal Society B: Biological Sciences*, 376 (1815). ISSN 0962-8436

<https://doi.org/10.1098/rstb.2019.0630>

© 2020 The Authors. This is an author-produced version of a paper accepted for publication in *Phil. Trans. B: Biological Sciences*. Uploaded in accordance with the publisher's self-archiving policy.

Reuse

Items deposited in White Rose Research Online are protected by copyright, with all rights reserved unless indicated otherwise. They may be downloaded and/or printed for private study, or other acts as permitted by national copyright laws. The publisher or other rights holders may allow further reproduction and re-use of the full text version. This is indicated by the licence information on the White Rose Research Online record for the item.

Takedown

If you consider content in White Rose Research Online to be in breach of UK law, please notify us by emailing eprints@whiterose.ac.uk including the URL of the record and the reason for the withdrawal request.



eprints@whiterose.ac.uk
<https://eprints.whiterose.ac.uk/>

More than just summed neuronal activity: how multiple cell types shape the BOLD response

Clare Howarth^{1}, Anusha Mishra^{2**}, Catherine Hall^{3**}**

¹Department of Psychology, University of Sheffield, Sheffield, S1 2LT, UK

²Department of Neurology, Jungers Center for Neurosciences Research and Knight Cardiovascular Institute, Oregon Health & Science University, Portland, OR 97239, USA

³School of Psychology, University of Sussex, Brighton, UK

^ These authors contributed equally to this work

*Address correspondence to Dr Clare Howarth, Department of Psychology, University of Sheffield, Cathedral Court, 1 Vicar Lane, Sheffield, S1 2LT, UK. Email: c.howarth@sheffield.ac.uk; Dr Anusha Mishra, Department of Neurology Jungers Center for Neurosciences Research and Knight Cardiovascular Institute, Oregon Health & Science University, Portland, OR 97239, USA. Email: mishraa@ohsu.edu or Dr Catherine Hall, School of Psychology, University of Sussex, Brighton, UK. Email: Catherine.Hall@sussex.ac.uk

Running title: Cellular mechanisms underlying BOLD

Abstract

Functional neuroimaging techniques are widely applied to investigations of human cognition and disease. The most commonly used among these is blood oxygen level-dependent (BOLD) functional magnetic resonance imaging (fMRI). The BOLD signal occurs because neural activity induces an increase in local blood supply to support the increased metabolism that occurs during activity. This supply usually outmatches demand, resulting in an increase in oxygenated blood in an active brain region, and a corresponding decrease in deoxygenated blood, which generates the BOLD signal. Hence, the BOLD response is shaped by an integration of local oxygen use, through metabolism, and supply, in the blood. To understand what information is carried in BOLD, we must understand how several cell types in the brain – local excitatory neurons, inhibitory neurons, astrocytes and vascular cells (pericytes, vascular smooth muscle, and endothelial cells), and their modulation by ascending projection neurons - contribute to both metabolism and haemodynamic changes. Here, we review the contributions of each cell type to the regulation of cerebral blood flow and metabolism, and discuss situations where a simplified interpretation of the BOLD response as reporting local excitatory activity may misrepresent important biological phenomena, for example with regards to arousal states, ageing and neurological disease.

Keywords

BOLD fMRI, neurovascular coupling, neurometabolic coupling, astrocyte, interneuron, endothelial propagation

The blood oxygen level-dependent (BOLD) signal in functional magnetic resonance imaging (fMRI) is used as a surrogate measure of neuronal activity. However, because it is not caused directly by neuronal activity but by the disruption of the magnetic field by deoxyhaemoglobin in the blood, the BOLD signal is influenced by several factors beyond neuronal activity. These factors include the geometry of the vascular bed with respect to the magnetic field [1], the concentration of haemoglobin in the blood, blood volume, and the oxygenation state of the blood. While the oxygenation state of the blood can be altered by systemic factors such as cardiac rhythm and breathing [Das et al., this issue], oxygenation state within the brain is set by the balance between extraction of oxygen from the blood to fuel increased metabolism (neurometabolic coupling), and the supply of freshly oxygenated blood to an active brain region due to the dilation of local blood vessels (neurovascular coupling, producing functional hyperaemia). In this review, we examine the contribution of different cell types to these two processes and, therefore, to the BOLD signal to better understand what a regional change in BOLD reveals about underlying neuronal activity.

Part 1: Neurovascular coupling

Why does neurovascular coupling exist? The brain is energetically expensive, accounting for 20% of the body's resting energy consumption [2]. In the cerebral cortex, the largest component of this energy is used to fuel the sodium-potassium ATPase, which reverses passive ion fluxes during action and synaptic potentials to maintain ionic electrochemical gradients [3,4]. Despite this high demand, the brain stores very low levels of energy substrates, largely in the form of glycogen, required for ATP production. Compared to other organs, the brain's glycogen storage capacity is approximately 1/10th of that of skeletal muscle and 1/30th that of liver (from values reported in [5–9]). Therefore, the brain requires a constant supply of oxygen and glucose to drive ATP production, mostly from oxidative phosphorylation [10]. Neurovascular coupling is assumed to be necessary to increase the supply of energy

substrates (oxygen and glucose) in the blood, when neurons are active. In fact, the supply of oxygen during neurovascular coupling is substantially greater than that consumed by active brain regions (e.g., [11–14]), at least in neocortex, resulting in the decrease in deoxygenated haemoglobin that produces the positive BOLD signal commonly measured in fMRI studies [15]. The reason for this oversupply of oxygen remains unclear, but may involve a requirement for a large concentration gradient between the vessel and the tissue for adequate oxygen delivery [16], and the spread of hyperaemia (increased blood supply) to vessels in regions that are not themselves active but that surround and are upstream of active brain regions (see below). Alternatively, the main purpose of neurovascular coupling may not be to increase oxygen supply [17,18] but something else, such as the maintenance of stable tissue glucose concentrations to support aerobic glycolysis [19] (but also see [20], [21]), washout of waste products such as CO₂ (but see [22]) and lactate (discussed in [23]), maintenance of appropriate tissue [O₂]/[CO₂] ratio [Buxton, this issue], or temperature regulation [24]. Whatever its purpose, the regional increase in oxygenated blood generated by neurovascular coupling is reliable enough, in healthy physiology, to generally allow an inference of increased neuronal activity from BOLD fMRI signals. However, an understanding of which cells drive the increase in cerebral blood flow (CBF, Figure 1) and which cells consume oxygen is required to fully and accurately interpret BOLD signals and to understand the limits of their utility.

Neuronal subtypes. Neuronal activity is the initiator of the BOLD signal, which is often assumed to represent the aggregate activity of excitatory neurons in a brain region. Indeed, task-associated BOLD signals increase in areas of the brain where excitatory activity is expected to be increasing [25–28]. Furthermore, studies combining electrophysiological recordings or specific inhibitors of neural activity with BOLD signals [28] and haemodynamic increases [29,30] have directly demonstrated that these measures reflect an underlying increase in net neural activity. Conversely, negative BOLD responses in human subjects were observed in regions exhibiting increased GABAergic tone [31], and thus where neuronal activity may have decreased below baseline levels. The idea that increased inhibition, and

thus lower net neural activity, underlies negative BOLD responses is further supported by experiments in primates [32] and rodents [33–36], which show that negative BOLD and haemodynamic signals occur in areas with decreased excitatory activity [37]. While this simple interpretation, that positive and negative BOLD signals reflect increases and decreases in net activity, lends itself easily to investigations of cognitive function in humans, it may not always hold true. Pharmacological studies blocking both glutamate and γ -aminobutyric acid (GABA) receptors have shown that both neurotransmitters are likely involved in neurovascular coupling [30,38,39]), suggesting that haemodynamic responses (and, therefore, the BOLD signal) are elicited by a combination of signals from excitatory and inhibitory neurons. Indeed, inhibitory interneurons may play a more important role in the production of BOLD signals than was previously appreciated. Many classes of interneurons have processes that directly target blood vessels [40] and can induce or modify neurovascular coupling [41]. Emerging evidence also indicates that inhibitory neurons can directly alter cerebral haemodynamics [42–46] in a manner that can be independent of net local activity [45,47]. In particular, using an optogenetic approach, Lee et al. [45] demonstrated that neuronal nitric oxide synthase (nNOS) expressing interneurons can drive increases in blood volume with minimal change in net neural activity. Activity in different interneuron populations might also generate the negative BOLD response: optogenetic activation of somatostatin [45] and parvalbumin [42,48] expressing interneurons can elicit “negative” haemodynamic responses. However, the contribution of these interneurons to the BOLD response is ambiguous, with studies reporting their ability to evoke positive [42,44,45], inverted [42,45,48], and delayed positive [44,46] haemodynamic responses. While the relative importance of individual subpopulations of inhibitory interneurons in shaping neurovascular coupling remains an open question, it is clear that these cells can directly modulate CBF and that BOLD signals reflect aspects of both excitatory and inhibitory neuronal activity. Therefore, although BOLD signals indicate changes in neural activity in specific brain regions, they cannot distinguish between increases in inhibitory and excitatory activity (see [49] for an in-depth discussion). Further, interneuron dysfunction is emerging as an important contributor to neurological and psychiatric diseases such as

Alzheimer's disease, epilepsy and schizophrenia (see [50–54]), which may alter neurovascular coupling and complicate interpretation of the BOLD response in these patient populations.

Task-induced activations may modulate subjects' attention and arousal via the activity of subcortical projection neurons such as neuromodulatory volume transmission systems (noradrenaline, acetylcholine, dopamine, serotonin etc.), which also modulate neurovascular coupling [55–57] and the BOLD signal [58–60]. These neuromodulatory systems can alter, independently, the activity of excitatory neurons, inhibitory interneurons, astrocytes, and even the vasculature itself, potentially complicating interpretation of BOLD signals during states of altered attention or arousal, or during diseases that affect these systems. A key question is whether the sensitivity of the vasculature to ongoing neural activity is altered by changes in neuromodulatory activity. This appears to be the case for the cholinergic system, as pharmacological or neurotoxic decreases in cholinergic tone weakened the correlation between sensory-evoked neuronal activity and the haemodynamic response [55]. Similar changes may contribute to the impaired neurovascular coupling [61] and BOLD signals [62–64] in Alzheimer's disease, a condition characterized by loss of cholinergic tone [65].

Astrocytes. Astrocytes are in contact with both neuronal synapses and blood vessels, ideally situating them to support neuronal energy demands: either directly through provision of metabolites such as lactate (reviewed by [66]; see below) or indirectly by involvement in neurovascular coupling (reviewed by [67]).

Neuronal activity can evoke an increase in astrocyte intracellular calcium, leading to release of vasoactive molecules, and altered haemodynamics [68–72]. Optogenetic stimulation of astrocytes can also increase BOLD without altering neuronal activity [73], indicating that astrocytes *can* act as a bridge between neuronal activity and blood flow. However, astrocytic calcium signals have been criticized as being too slow or infrequent to explain the dilations of

arterioles that occur in response to neural activity [68,74–76]. Instead, these slow, usually somatic, increases in astrocyte calcium may: (a) contribute to arteriolar dilation only under conditions of sustained neuronal activity [75,77], (b) mediate vasoconstriction and the return to baseline tone after functional hyperaemia [78], and (c) modulate basal vessel tone [75,79,80]. Astrocytes may also facilitate neurovascular coupling, as slow increases in astrocyte calcium may produce longer duration [77] haemodynamic responses.

In contrast to these slow calcium signals, fast calcium signals associated with neural/synaptic activity in (predominantly) astrocytic fine processes and endfeet are increasingly being reported [78,81–83]. These signals occur shortly after neural activity [84,85], precede arteriole and capillary dilation [86] and potentiate the increase in blood volume by almost 3-fold [78]. These fast signals may be particularly important for controlling flow in the capillary bed, where (unlike in arterioles) astrocyte calcium signals were found to be necessary for neurovascular coupling [69,70].

In summary, astrocytes may drive neurovascular coupling in two ways: fast calcium signals that fine-tune the haemodynamic response by generating molecules that dilate capillaries, and slow calcium signals that modulate the size and shape of arterial dilations, and perhaps help terminate functional hyperaemia when neuronal activity ceases. The specific features of neuronal activity that drive these different astrocyte signals are currently unclear, and their discovery will be key for fully understanding what information haemodynamic and BOLD signals carry about neuronal activity changes. Furthermore, because spin echo signals reflect changes in capillaries more robustly than gradient echo signals, particularly at higher magnetic fields [87–89], and because capillary dilations depend on fast astrocyte signals, fMRI experiments may differentially reflect certain aspects of neuronal and astrocyte activity depending on the methodology used.

Lastly, the role of astrocytes in shaping the BOLD signal in neurological diseases must also be considered. In Alzheimer's disease and following ischemia, subarachnoid haemorrhage, and traumatic brain injury, impairments in neurovascular coupling and cerebral haemodynamics have been reported in both humans and animal models [90,91]. These same conditions are also characterized by reactive astrogliosis, a response of astrocytes to alterations in their microenvironment that includes changes in their morphology and gene expression. It is conceivable that reactive astrocytes are, at least in part, to blame for the neurovascular deficits in these conditions [90,92] and should be the focus of future research. For example, subarachnoid haemorrhage causes an inversion of neurovascular coupling, whereby increases in neural activity are coupled to a decrease in CBF, which are mediated by pathologically large calcium signals within astrocyte endfeet causing a large outflux of potassium, via BK channels, onto the vasculature [93]. Interpretation of the BOLD response from patient populations should therefore consider such astrocyte-mediated uncoupling between neural activity and CBF.

The vasculature. In addition to signals from neurons and astrocytes, properties of the vasculature itself shape the BOLD response in multiple ways. While anatomical differences in vascular beds (geometry relative to the magnetic field, vascular density, proportion of veins and capillaries) can alter the magnitude of the BOLD signal (see [1,16,94,95]), we focus here on the contributions of different cell types to the physiological processes that underpin BOLD.

Vascular mural cells: pericytes and smooth muscle cells. The cells that directly constrict and dilate blood vessels by contracting or relaxing in response to signals from the parenchyma, or the blood, are the contractile vascular mural cells: smooth muscle cells (SMCs) and pericytes. The definitions of these two types of cells have been hotly debated [96,97], but here we consider pericytes as mural cells with discrete soma and processes, and SMCs as cells with a banded and contiguous morphology [97]. SMCs on arterioles have long been known to be involved in mediating vascular dilations that underlie neurovascular

coupling, whereas the role of pericytes on capillaries and precapillary arterioles has emerged more recently [70,98–100]. Pericyte morphology varies down the vascular bed, as has been elegantly described [101], from ensheathing pericytes, whose processes encircle the underlying vessel, to thin-strand pericytes in the middle of the capillary bed, with long processes that extend along but rarely around the vessel. It is now well-established that ensheathing pericytes express smooth muscle actin and can actively constrict and dilate in response to neuronal activity [96,99,101,102]. More controversial is whether mesh and thin strand pericytes on smaller capillaries can regulate vessel diameter. Although some groups find they do not [96,103], neuronal activation causes calcium to drop in these cells [102], and we and others have observed capillary dilations in response to neuronal activity (up to 4th branching order, $\leq 5 \mu\text{m}$ [70,99,100,102,104]), and two recent papers report constriction of mid-capillary pericytes in response to optogenetic stimulation [105,106]. We suspect that the imaging resolution, sampling rate and smoothing may be key factors in whether these small fluctuations in diameter in the mid-capillary bed can be detected. The evolutionary reason for such local regulation of blood flow is unclear. Perhaps active neurons' oxygen requirements are best matched by very local modulation of blood flow, or perhaps local regulation is simply a consequence of local production of vasoactive signalling molecules with a limited diffusional spread. Alternatively, capillary-level regulation of flow could optimise tissue oxygenation by allowing the increase in homogeneity of red blood cell flux in different capillaries that happens during functional activation [107,108], which maximises oxygen extraction [109,110].

The responses of all of these different types of pericytes are important for shaping the increase in CBF that occurs following neuronal activity. Because capillaries represent a higher resistance to flow than arterioles or venules [111], their dilation produces a larger decrease in resistance than does arteriole dilation. Therefore, relaxation of capillary pericytes mediates a larger component of the functional hyperaemia response (capillary dilation contributes to 50-84% of the overall change in CBF, while arteriole dilation contributes $< 25\%$ [99,102]). The speed at which different types of pericytes respond to neuronal activation varies, with

ensheathing pericytes on the first and second branches off an arteriole dilating before downstream mid-capillary pericytes [99,102,112]. The relative response times of first order branches compared to upstream arterioles is less clear, with different studies reporting that first order branches dilate earlier than [99,112], concurrently with [102] or following [113,114] the upstream arterioles. Regardless of timing, these dilations are functionally important: using a compartmentalized computational model, Rungta et al. [102] demonstrated that the absence of dilation by either ensheathing or mid-capillary pericytes profoundly attenuates evoked increases in CBF. Thus, the BOLD signal is shaped in different ways by ensheathing pericytes - the likely initiators of capillary dilation - and mid-capillary thin strand pericytes, whose dilation mediates the majority of the increase in flow.

These vascular mural cells might also be differentially sensitive to disease. For example, in Alzheimer's disease, soluble A β constricts pericytes [115], whereas its effect on smooth muscle cells is more debated [115–117]. Cerebral amyloid angiopathy, on the other hand, in which A β aggregates deposit on vessels, preferentially occurs around the smooth muscle cells of larger arterioles [118] and restricts their function [119]. Thus, BOLD signals in patients with Alzheimer's disease might be compromised differently depending on the disease state, due initially to effects on pericytes by soluble A β , and later on smooth muscle cells by aggregates of A β that form around arterioles.

Endothelial cells. The best-established role of endothelial cells in shaping the vascular response to neuronal activity, and therefore the BOLD signal, is to propagate vasodilatory signals along the vasculature, thus amplifying the haemodynamic response by dilating blood vessels upstream of local neural activity. Such long-range propagation and modulation of blood flow has long been known to occur in peripheral vascular beds [120,121], the retina [122], and the brain [123], although the mechanisms that underlie this propagation and how this shapes neurovascular coupling have only recently been appreciated [124,125]. Vasodilation arising from neuronal activity local to the mid-capillary bed can be communicated

to upstream vessels by a regenerating hyperpolarising current that is mediated by Kir2.1 channels [103] and propagated between endothelial cells via connexin-40 containing gap junctions [126], which couple more efficiently and preferentially towards upstream vessels during functional activation [127]. Activation of endothelial NMDA receptors and endothelial NOS (eNOS) can also evoke dilation in adjacent vascular mural cells [128,129]. Given the evidence discussed in previous sections, it is likely that these signals first produce vasodilation in ensheathing pericytes of small arterioles or first capillary branches before being propagated upstream to dilate larger penetrating and pial arterioles. Whether dilation of mid-capillary pericytes occurs as a slowly developing response to the same vasoactive signal that generates a propagating hyperpolarisation of endothelial cells, or as a secondary passive response to the upstream dilation remains to be seen.

Vasoactive signals propagated through the endothelium shape functional hyperaemia, and therefore BOLD signals. The haemodynamic response to neural activity (particularly in the first 10 s of a 12 s hindpaw stimulation) was reduced when endothelial signalling and, therefore, propagation of vasodilation, was prevented by light-dye treatment of pial arteries [130]. Endothelial propagation also gives rise to another interesting phenomenon: once vasodilation has spread upstream to pial arteries, it can then propagate down other vessel branches that feed nearby brain regions that do not themselves harbour any change in neuronal activity [131,132], leading to two important features of the BOLD signal. First, the early haemodynamic response (<2 s) is more spatially confined to the active region of the brain compared to the later component, as the signal has not had time to propagate outside the active region [133]. Second, the propagated increase in blood flow is likely to be a major reason why the positive BOLD signal exists: inactive tissue near activated regions experiences an increase in blood supply without any oxygen consumption, allowing the oxygenated haemoglobin levels to increase and deoxyhaemoglobin levels to fall, thereby generating the positive BOLD signal. This idea is supported by optical intrinsic imaging and spectroscopic studies that identified a small region of tissue hypoxia and increased oxygen consumption in the active region,

immediately before oxygenated blood volume increased in the surrounding area spanning several millimeters [134,135]. This localized increase in oxygen consumption prior to the CBF increase gives rise to the 'initial dip' sometimes observed in the BOLD signal with a similar spatial and temporal pattern [133,136–138].

BOLD signals can also be shaped by multiple factors that modulate endothelial propagation of vasodilation. In the retina, endothelial conduction is dramatically reduced by the vasoconstricting hormone angiotensin II [139], and facilitated by nitric oxide (NO) [127]. In the cortex, neurovascular coupling depends on arterial endothelial cell caveolae, which may be required to cluster the ion channels required for propagation [140]. Endothelial propagation may also be modulated by changes in levels of the membrane phospholipid PIP2 which, when depleted by activation of Gq-coupled receptors, reduce activity of Kir2.1 and impair propagation of vasodilation [141]. Many of these pathways are modified by disease. Loss of endothelial or pericyte-endothelial gap junction coupling is observed in diabetes [122,127,142], while angiotensin II levels are raised in hypertension [139] and angiotensin II synthesis and its receptor are primary targets of hypertension treatment [143]. These pathologies, or treatments thereof, are likely to regulate endothelial cell coupling and thus the spread of dilation through the vascular network, ultimately influencing the size and shape of the BOLD response. Consideration of impaired functioning of pericytes, smooth muscle cells and endothelial cells is therefore critical when conducting BOLD experiments in ageing and patient populations.

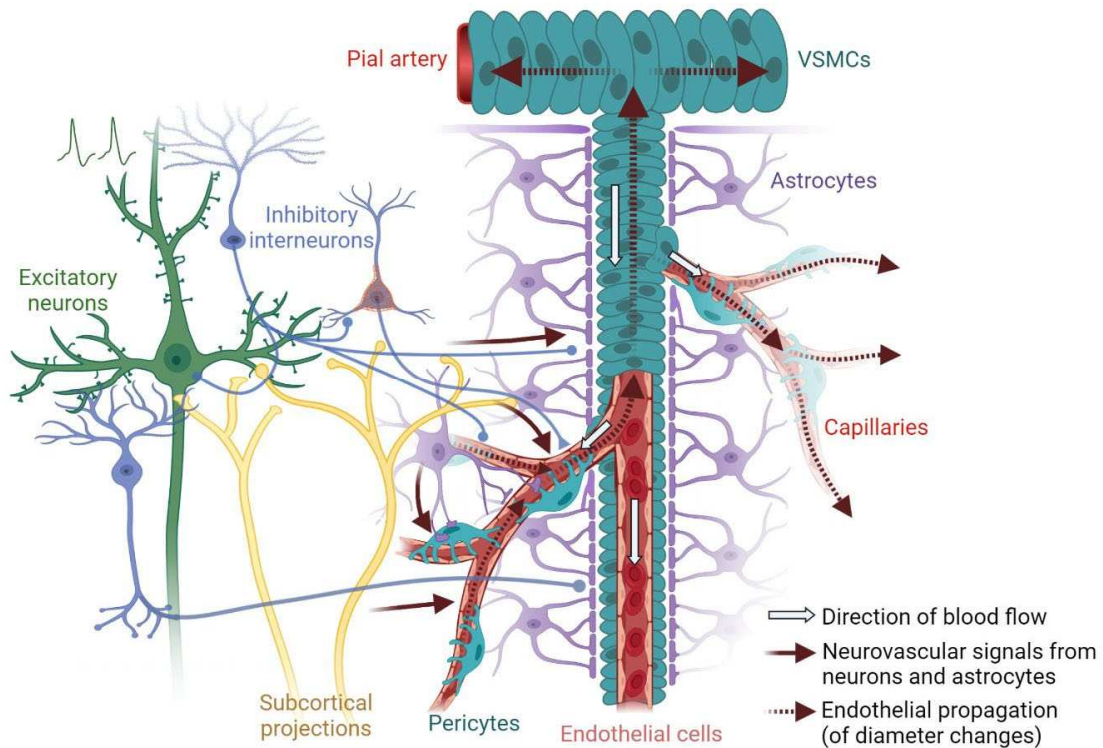


Figure 1. Multicellular contributions to neurovascular coupling.

Activation of excitatory neurons in the brain is believed to initiate the neurovascular signals that cause increases in cerebral blood flow (CBF). However, inhibitory interneuron activity almost invariably occurs in parallel with excitatory activity and signals from these interneurons appear to be the stronger regulators of cerebral blood flow. Neural activity also stimulates astrocytes, which can regulate capillary diameter and modulate overall changes in CBF. Ascending projection systems can further tune the locally generated vasoactive signals, or may directly modulate the vasculature. Once the vascular pericytes or endothelial cells have sensed vasoactive signals from the surrounding tissue, these signals propagate through the endothelium to contractile pericytes and smooth muscle cells on upstream vessels and their branches, which may not themselves feed active tissue. Created with [BioRender.com](https://www.biorender.com).

Part 2: Contributions of Metabolism to BOLD

As discussed above, the increase in CBF that irrigates active brain regions occurs in response to concerted signalling from several cell types including excitatory neurons, inhibitory neurons and astrocytes. Haemodynamic responses are further shaped by modulation from subcortical structures, and endothelial propagation along the vascular tree. However, the BOLD response represents not only the increase in oxygenated blood but its balance with the rate of oxygen consumption by nearby cells. Therefore, it is important to consider the oxygen consumption of different cell types in the brain to determine their relative impact on the BOLD signal. Neglecting any roles in increasing blood flow, highly oxygen-consuming cells will reduce blood oxygenation and the positive BOLD signal, so using positive BOLD as a readout of neuronal activity will underrepresent these signals compared to active, but less oxygen-consuming cells. These cells' activity will be better detected using calibrated BOLD methods, which allow the calculation of regional oxygen consumption rates by disambiguating changes in CBF from the BOLD response [144].

Oxygen consumption by different cell types

Excitatory neurons. Energy budgets of neuronal transmission, which calculate the expected ATP use of different cellular processes based on membrane conductances, firing rates and sizes of different cell types, initially suggested that action potentials accounted for the majority of signalling energy use within rodent cortical grey matter [3]. However, incorporating energetically efficient action potentials [145,146] into such calculations results in excitatory synapses being the most energetically expensive component of neuronal signalling [4]. This is because of the relatively large ion fluxes that drive excitatory postsynaptic potentials (EPSPs) compared to action potentials, which then need to be reversed by action of the sodium-potassium ATPase. The proportion of energy use associated with various cortical signalling processes has been suggested to be consistent across mammalian species and activity levels, with post-synaptic processes being the largest consumers of neuronal ATP in

both rodents (47-53%) and humans (42-59%) [147]. These findings support the use of rodent models in fMRI studies informing our knowledge of human brain function. Careful cross-species approaches will allow more reliable translation of findings between preclinical and human fMRI studies [Barron et al., this issue].

ATP at synapses is proposed to be glycolytically generated [148], and therefore not to consume oxygen or influence the BOLD signal. However, measurements of oxygen concentrations during inhibition of glutamatergic synapses showed that most oxygen was consumed by EPSPs at synapses, followed by action potentials [10], and that correlations between LFP size and cerebral metabolic rate of O₂ (CMRO₂) [149,150] support excitatory synapses as a crucial determinant of CMRO₂. Because there are nine times more excitatory than inhibitory neurons in the cerebral cortex [151] and because excitatory neurons have more excitatory synapses than do interneurons [152], much of the oxygen consumed by EPSPs and action potentials will be used by excitatory cells. Hence, it follows that excitatory neurons are a major consumer of tissue oxygen.

Inhibitory neurons. While fewer in number, inhibitory neurons may still contribute to brain oxygen consumption in two substantial ways; first, by increasing the energetic cost of excitation and second, by being, on average, more metabolically active than excitatory neurons [153].

Inhibitory inputs can increase the energetic costs of excitatory cells' firing. Reversal of chloride fluxes at inhibitory synapses is, in itself, not expected to be energetically expensive as the reversal potential for chloride is near the resting membrane potential of the cell. However, the co-occurrence of excitation and inhibition may increase the energetic cost of excitation in at least two ways. Firstly, inhibition increases the metabolic cost of excitatory synapses: by holding the membrane at more hyperpolarised potentials, inhibition increases the driving force and inward flux of sodium ions, which then require more ATP to reverse these ion fluxes [154].

Secondly, in the presence of inhibition, more excitatory inputs are required for a cell to reach its threshold for firing an action potential. This happens because excitation needs to counter both hyperpolarisation of the membrane and shunting inhibition - the increased membrane conductance caused by opening of chloride or potassium channels that impairs the spread of EPSPs to the axon hillock. The increased sodium driving force and requirement for more synaptic inputs both critically depend on the timing of inhibitory inputs, with increased temporal overlap between inhibitory and excitatory inputs to a single cell predicted to dramatically impact the energy cost of neuronal transmission [154]. In fact, inhibitory and excitatory inputs to hippocampal and cortical neurons are often near-synchronous during fast sharp wave ripple [155,156], theta-like [157] and slow (<1 Hz) oscillations [158], suggesting that inhibition is likely to increase the energy used to fuel excitatory neurons in these conditions. This “tight balance” of excitation and marginally delayed inhibition to individual principal neurons is a common (though not universal) feature of neural networks, which increases the precision of spike timing and makes coding more efficient by reducing the number of spikes needed to accurately represent information at the population level [159]. Thus, brain networks may offset increased synaptic energy use caused by concurrent excitation and inhibition with resultant decreased energy spent on spiking per unit of information transmitted.

The degree of overlap of excitation and inhibition is not constant at a synapse, suggesting that the metabolic cost of inhibition will also vary. At CA3-CA1 synapses, Bhatia et al. found no overlap between EPSCs and IPSCs in response to activation of only a few synapses, while stronger stimuli evoked faster IPSCs that overlapped with EPSCs [160]. Therefore inhibition is expected to disproportionately increase synaptic energy use for stronger stimuli in this network, potentially reducing the size of the positive BOLD response to such stimuli (which would be better represented by CMRO₂ measurements from calibrated BOLD). Factors that alter inhibition, such as alterations in brain state and the neuromodulators acetylcholine and noradrenaline [161,162], are also likely to affect the degree of overlap of inhibitory and excitatory currents, and therefore the synaptic energy use. The contribution of inhibitory

currents to excitatory synaptic energy use is therefore likely to be quite variable and altered in different arousal states or disease, but requires quantification before it is possible to estimate its effect on net CMRO₂ or BOLD.

In addition to the impact of inhibition on the metabolic cost of excitatory synaptic inputs, increased energy use due to inhibition may occur due to oxygen consumption by inhibitory interneurons themselves. Fast-spiking parvalbumin interneurons are probably the main contributor to increased energy metabolism during inhibition. They are relatively numerous (around 40% of GABAergic cells in neocortex, for example [163]) and relative to other interneurons, they have higher levels of cytochrome c oxidase, more mitochondria, a higher density of excitatory inputs and adaptations such as increased sodium channel density, which allows an extremely fast firing rate but decreases the energy efficiency of action potential firing [164–166]. The contribution of other interneuron types to net CMRO₂ is less studied, but may also be significant (although see [167]), as their firing rates and cytochrome c oxidase levels can be higher than those in pyramidal cells [164,165]. In contrast to excitatory neurons, interneurons are generally expected to consume more oxygen to fuel action potentials than synaptic potentials, because of their lower dendritic complexity but increased axonal length and branching [168] (but also see [147]). Notably, the populations of interneurons that are likely to make the largest contribution to brain oxygen consumption may not be the same as those that control blood flow: Fast spiking parvalbumin cells are very metabolically active, but may not play a major role in control of blood flow, while nNOS-positive interneurons can control blood flow but make up only 20% of all interneurons [40] and 2% of all neurons [169], and hence are likely to be relatively underrepresented in CMRO₂. Therefore, positive BOLD and calibrated BOLD measurements provide very different information about which types of inhibitory cells are active.

Experimentally, inhibition has been shown to have a significant energetic cost. 2-deoxyglucose uptake (and by extrapolation, metabolism) was more correlated with the degree of inhibition

than pyramidal cell firing after electrical stimulation of hippocampal inputs in rats [170]. Similarly, in rat dentate gyrus, low frequency stimulation of the perforant path decreased EPSP slope and population spike latency (suggesting increased inhibitory tone), and decreased BOLD, but CBV was relatively preserved. This indicated that $CMRO_2$ was elevated by the increased inhibition [171]. These studies therefore suggest that $CMRO_2$ is not necessarily a good indicator of principal (excitatory) neuron activity, but also represents inhibitory tone, be it altering the metabolic cost of information transmission within excitatory cells and/or the firing of inhibitory neurons themselves.

The impact of inhibition on $CMRO_2$ should make us reconsider the meaning of “activation” of a brain region. As discussed above, a key function of inhibition is thought to be to increase precision of spike timing, and it may not necessarily alter the net firing rate of a neuron. Therefore, fluctuations in inhibition during a cognitive process may alter coding and oxygen use in a brain region without altering the firing rate of principal neurons. From a computational perspective, this brain region is therefore involved in the cognitive process but its “activity” in classic terms of the level of excitatory input or output has not changed. Maybe, then, it would be better to consider our aim with functional imaging to detect regions of altered processing, rather than of activation? In this example, where inhibition alters spike timing but not spike rate, $CMRO_2$ measurements would allow us to detect the changes in processing. However, blood flow may not change (depending on whether the interneurons mediating inhibition can dilate vessels) and positive BOLD could be increased, decreased or unchanged, depending on the level of any increased energy use and any increase (or not) in CBF.

Glial cells. Metabolism in astrocytes, oligodendrocytes, or vascular cells might also be expected to vary with neuronal activity, but, in fact, they probably do not contribute much to the corresponding fluctuations in $CMRO_2$. Astrocytes contain mitochondria and consume oxygen when depolarised optogenetically [73]. However, their metabolism is thought to be predominantly glycolytic [172], and blocking astrocytic oxidative phosphorylation does not

affect net CMRO₂ [173]. Indeed, active neurons may actually trigger increased glycolytic ATP production in astrocytes to a degree that inhibits astrocytic oxidative phosphorylation, in order to boost oxygen availability for neurons [174]. Lactate produced by glycolysis in astrocytes may then be shuttled to neurons to support their oxidative metabolism [172]. The degree of contribution of this astrocyte-neuron lactate shuttle in fuelling the increased neuronal activity remains controversial [175], however, in part because astrocytic glycolysis occurs after neuronal oxidative phosphorylation [176].

Mature oligodendrocytes consume very little oxygen as their metabolism is predominantly glycolytic, while oligodendrocyte precursor cells (OPCs) produce ATP predominantly via oxidative phosphorylation [177]. However, oxygen use by OPCs associated with increased neuronal activity is likely minimal. Although their resting energy consumption in white matter is similar to that in the grey matter, their activity-dependent ATP use (synaptic connections from axons to OPCs) is <1% of the total cost of neuronal signalling in grey matter [178].

Vasculature. The amount of oxygen consumed by the brain's vasculature (endothelial cells, smooth muscle cells and pericytes) itself is a question that deserves further study. The maintenance of resting vascular tone, as well as changes therein during neurovascular coupling, are enacted by the movement of ions, particularly calcium and potassium, across the membrane of these vascular cells. ATP is required to re-establish these ionic gradients and, therefore, vascular activity is expected to increase metabolism. Experiments performed outside the nervous system suggest that these cells are highly energy consumptive. Sizeable drops in oxygen concentration have been recorded across the vessel wall of mesenteric and pial arteries, and models suggest this reflects significant oxygen consumption by smooth muscle and endothelial cells rather than just the existence of a diffusion barrier [179,180]. Studies in dog and pig aorta have found a significantly higher rate of oxygen consumption at the luminal/endothelial surface compared to the abluminal surface (0.36 mM/min vs. 0.016 mM/min [181]), indicating that endothelial cells contribute significantly to vascular consumption

rates. The drop in oxygen concentration across the vessel wall also increases with increased wall thickness, or decreasing branching order of the vessel, suggesting that the number of layers of vascular mural cells also play a role [180]. At 1-5 mM/min O_2 , net $CMRO_2$ of the brain [182,183] is much higher than the oxygen consumption rate of the vasculature measured by some groups [181], though others find higher values (up to 10 mM/min [179]). However, because the volume fraction of the brain's vasculature is only 1-3% [184], the contribution of vascular cells to net $CMRO_2$ is likely minimal compared to that of neurons, though it may significantly affect O_2 concentrations close to vessels.

In summary, brain oxygen consumption is predominantly due to excitatory and inhibitory neuronal activity, although glial and vascular cells also contribute. Oxygen consumption by active neurons reduces positive BOLD signals, confounding the accuracy of positive BOLD as a readout of neuronal activity. $CMRO_2$ measurements from calibrated BOLD studies may be a more accurate read out of the level of net neuronal activity than positive BOLD, as they are more spatially localised to active brain regions. However, because the cells that are the most metabolically active (excitatory neurons or parvalbumin interneurons) are likely not the same cells that signal to blood vessels to dilate (likely nNOS-positive inhibitory neurons or astrocytes), $CMRO_2$ signals carry different information about which cells are active than do positive BOLD signals.

Conclusion

BOLD signals are shaped by the balance between oxygen supply and its consumption. Extracting the maximum amount of accurate information from BOLD signals will require understanding which cells' activity shapes these two processes, especially as the same cells are not equally responsible for both processes. For example, active nNOS-positive interneurons can dilate the vasculature, but are unlikely to contribute substantially to oxygen consumption, while parvalbumin interneurons contribute much more to oxygen consumption

but are less likely to drive increases in CBF. Astrocytes can initiate vascular responses at smaller vessels while modulating the response of arterioles, and vascular mural and endothelial cells detect and propagate these signals to amplify the haemodynamic response ultimately measured by BOLD, without contributing as much to oxygen consumption. A nuanced understanding of how alterations in excitatory-inhibitory balance and different interneuron populations affect oxygen supply and consumption is key to discovering how BOLD signals relate to circuit activity. Furthermore, future interpretation of BOLD signals should also reflect our increasing understanding of how neurons, astrocytes and vascular cells can be differentially affected by disease states, and have correspondingly different effects on BOLD.

Acknowledgements

Clare Howarth is funded by a Sir Henry Dale Fellowship jointly funded by the Wellcome Trust and the Royal Society (Grant Number 105586/Z/14/Z). Anusha Mishra is funded by Collins Medical Trust, NIH NINDS (1R01NS110690), NIH NIMH (1R01DA047237) and NIH NIA (P30AG066518-01; Oregon Alzheimer's Disease Research Center, PI: Kaye). Catherine Hall is funded by the Medical Research Council (MR/S026495/1), the Royal Society (RGS\R1\191203) and the Alzheimer's Research UK South Coast Network.

References

1. Gagnon L, Sakadžić S, Lesage F, Musacchia JJ, Lefebvre J, Fang Q, et al. Quantifying the microvascular origin of BOLD-fMRI from first principles with two-photon microscopy and an oxygen-sensitive nanoprobe. *J Neurosci*. 2015;35: 3663–3675.
2. Sokoloff L. The metabolism of the central nervous system in vivo. *Handbook of Physiology*, section, I, Neurophysiology. 1960;3: 1843–1864.
3. Attwell D, Laughlin SB. An energy budget for signaling in the grey matter of the brain. *J Cereb Blood Flow Metab*. 2001;21: 1133–1145.
4. Howarth C, Gleeson P, Attwell D. Updated energy budgets for neural computation in the neocortex and cerebellum. *J Cereb Blood Flow Metab*. 2012;32: 1222–1232.
5. Oe Y, Baba O, Ashida H, Nakamura KC, Hirase H. Glycogen distribution in the microwave-fixed mouse brain reveals heterogeneous astrocytic patterns. *Glia*. 2016;64: 1532–1545.
6. Wasserman DH. Four grams of glucose. *Am J Physiol Endocrinol Metab*. 2009;296: E11–21.
7. Molina DK, DiMaio VJM. Normal organ weights in men: part II-the brain, lungs, liver, spleen, and kidneys. *Am J Forensic Med Pathol*. 2012;33: 368–372.
8. Holmes EG, Holmes BE. Contributions to the Study of Brain Metabolism: Carbohydrate Metabolism Relationship of Glycogen and Lactic Acid. *Biochem J*. 1926;20: 1196–1203.
9. Janssen I, Heymsfield SB, Wang Z, Ross R. Skeletal muscle mass and distribution in 468 men and women aged 18–88 yr. *J Appl Physiol*. 2000;89: 81–88.
10. Hall CN, Klein-Flugge MC, Howarth C, Attwell D. Oxidative Phosphorylation, Not Glycolysis, Powers Presynaptic and Postsynaptic Mechanisms Underlying Brain Information Processing. *Journal of Neuroscience*. 2012. pp. 8940–8951. doi:10.1523/jneurosci.0026-12.2012
11. Fox PT, Raichle ME. Focal physiological uncoupling of cerebral blood flow and oxidative metabolism during somatosensory stimulation in human subjects. *Proc Natl Acad Sci U S A*. 1986;83: 1140–1144.
12. Lecoq J, Tiret P, Najac M, Shepherd GM, Greer CA, Charpak S. Odor-evoked oxygen consumption by action potential and synaptic transmission in the olfactory bulb. *J Neurosci*. 2009;29: 1424–1433.
13. Parpaleix A, Goulam Houssen Y, Charpak S. Imaging local neuronal activity by monitoring PO₂ transients in capillaries. *Nat Med*. 2013;19: 241–246.
14. Sakadžić S, Yuan S, Dilekoz E, Ruvinskaya S, Vinogradov SA, Ayata C, et al. Simultaneous imaging of cerebral partial pressure of oxygen and blood flow during functional activation and cortical spreading depression. *Appl Opt*. 2009;48: D169–77.
15. Ogawa S, Lee TM, Kay AR, Tank DW. Brain magnetic resonance imaging with contrast dependent on blood oxygenation. *Proc Natl Acad Sci U S A*. 1990;87: 9868–9872.
16. Buxton RB. Interpreting oxygenation-based neuroimaging signals: the importance and

- the challenge of understanding brain oxygen metabolism. *Front Neuroenergetics*. 2010;2: 8.
17. Mintun MA, Lundstrom BN, Snyder AZ, Vlassenko AG, Shulman GL, Raichle ME. Blood flow and oxygen delivery to human brain during functional activity: theoretical modeling and experimental data. *Proc Natl Acad Sci U S A*. 2001;98: 6859–6864.
 18. Lindauer U, Leithner C, Kaasch H, Rohrer B, Foddiss M, Füchtmeier M, et al. Neurovascular coupling in rat brain operates independent of hemoglobin deoxygenation. *J Cereb Blood Flow Metab*. 2010;30: 757–768.
 19. Fox PT, Raichle ME, Mintun MA, Dence C. Nonoxidative glucose consumption during focal physiologic neural activity. *Science*. 1988;241: 462–464.
 20. Powers WJ, Hirsch IB, Cryer PE. Effect of stepped hypoglycemia on regional cerebral blood flow response to physiological brain activation. *Am J Physiol*. 1996;270: H554–9.
 21. Angleys H, Østergaard L, Jespersen SN. The effects of capillary transit time heterogeneity (CTH) on brain oxygenation. *J Cereb Blood Flow Metab*. 2015;35: 806–817.
 22. Pinard E, Tremblay E, Ben-Ari Y, Seylaz J. Blood flow compensates oxygen demand in the vulnerable CA3 region of the hippocampus during kainate-induced seizures. *Neuroscience*. 1984;13: 1039–1049.
 23. Raichle ME. Behind the scenes of functional brain imaging: a historical and physiological perspective. *Proc Natl Acad Sci U S A*. 1998;95: 765–772.
 24. Sukstanskii AL, Yablonskiy DA. Theoretical model of temperature regulation in the brain during changes in functional activity. *Proc Natl Acad Sci U S A*. 2006;103: 12144–12149.
 25. Logothetis NK, Guggenberger H, Peled S, Pauls J. Functional imaging of the monkey brain. *Nature Neuroscience*. 1999. pp. 555–562. doi:10.1038/9210
 26. Marota JJ, Ayata C, Moskowitz MA, Weisskoff RM, Rosen BR, Mandeville JB. Investigation of the early response to rat forepaw stimulation. *Magn Reson Med*. 1999;41: 247–252.
 27. Silva AC, Lee SP, Yang G, Iadecola C, Kim SG. Simultaneous blood oxygenation level-dependent and cerebral blood flow functional magnetic resonance imaging during forepaw stimulation in the rat. *J Cereb Blood Flow Metab*. 1999;19: 871–879.
 28. Logothetis NK, Pauls J, Augath M, Trinath T, Oeltermann A. Neurophysiological investigation of the basis of the fMRI signal. *Nature*. 2001;412: 150–157.
 29. Berwick J, Johnston D, Jones M, Martindale J, Martin C, Kennerley AJ, et al. Fine detail of neurovascular coupling revealed by spatiotemporal analysis of the hemodynamic response to single whisker stimulation in rat barrel cortex. *J Neurophysiol*. 2008;99: 787–798.
 30. Lecrux C, Toussay X, Kocharyan A, Fernandes P, Neupane S, Lévesque M, et al. Pyramidal Neurons Are “Neurogenic Hubs” in the Neurovascular Coupling Response to Whisker Stimulation. *J Neurosci*. 2011;31: 9836–9847.

31. Northoff G, Walter M, Schulte RF, Beck J, Dydak U, Henning A, et al. GABA concentrations in the human anterior cingulate cortex predict negative BOLD responses in fMRI. *Nat Neurosci.* 2007;10: 1515–1517.
32. Shmuel A, Augath M, Oeltermann A, Logothetis NK. Negative functional MRI response correlates with decreases in neuronal activity in monkey visual area V1. *Nat Neurosci.* 2006;9: 569–577.
33. Boorman L, Kennerley AJ, Johnston D, Jones M, Zheng Y, Redgrave P, et al. Negative blood oxygen level dependence in the rat: a model for investigating the role of suppression in neurovascular coupling. *J Neurosci.* 2010;30: 4285–4294.
34. Boorman L, Harris S, Bruyns-Haylett M, Kennerley A, Zheng Y, Martin C, et al. Long-latency reductions in gamma power predict hemodynamic changes that underlie the negative BOLD signal. *J Neurosci.* 2015;35: 4641–4656.
35. Devor A, Tian P, Nishimura N, Teng IC, Hillman EMC, Narayanan SN, et al. Suppressed neuronal activity and concurrent arteriolar vasoconstriction may explain negative blood oxygenation level-dependent signal. *J Neurosci.* 2007;27: 4452–4459.
36. Kastrup A, Baudewig J, Schnaudigel S, Huonker R, Becker L, Sohns JM, et al. Behavioral correlates of negative BOLD signal changes in the primary somatosensory cortex. *Neuroimage.* 2008;41: 1364–1371.
37. Harel N, Lee S-P, Nagaoka T, Kim D-S, Kim S-G. Origin of Negative Blood Oxygenation Level—Dependent fMRI Signals. *J Cereb Blood Flow Metab.* 2002;22: 908–917.
38. Han K, Min J, Lee M, Kang B-M, Park T, Hahn J, et al. Neurovascular Coupling under Chronic Stress Is Modified by Altered GABAergic Interneuron Activity. *J Neurosci.* 2019;39: 10081–10095.
39. Shi Y, Liu X, Gebremedhin D, Falck JR, Harder DR, Koehler RC. Interaction of mechanisms involving epoxyeicosatrienoic acids, adenosine receptors, and metabotropic glutamate receptors in neurovascular coupling in rat whisker barrel cortex. *J Cereb Blood Flow Metab.* 2008;28: 111–125.
40. Tricoire L, Vitalis T. Neuronal nitric oxide synthase expressing neurons: a journey from birth to neuronal circuits. *Front Neural Circuits.* 2012;6: 82.
41. Cauli B, Tong X-K, Rancillac A, Serluca N, Lambolez B, Rossier J, et al. Cortical GABA interneurons in neurovascular coupling: relays for subcortical vasoactive pathways. *J Neurosci.* 2004;24: 8940–8949.
42. Lee JH, Durand R, Gradinaru V, Zhang F, Goshen I, Kim D-S, et al. Global and local fMRI signals driven by neurons defined optogenetically by type and wiring. *Nature.* 2010;465: 788–792.
43. Uhlirova H, Kılıç K, Tian P, Thunemann M, Desjardins M, Saisan PA, et al. Cell type specificity of neurovascular coupling in cerebral cortex. *Elife.* 2016;5. doi:10.7554/eLife.14315
44. Krawchuk MB, Ruff CF, Yang X, Ross SE, Vazquez AL. Optogenetic assessment of VIP, PV, SOM and NOS inhibitory neuron activity and cerebral blood flow regulation in

- mouse somato-sensory cortex. *J Cereb Blood Flow Metab.* 2020;40: 1427–1440.
45. Lee L, Boorman L, Glendenning E, Christmas C, Sharp P, Redgrave P, et al. Key Aspects of Neurovascular Control Mediated by Specific Populations of Inhibitory Cortical Interneurons. *Cereb Cortex.* 2020;30: 2452–2464.
 46. Dahlqvist MK, Thomsen KJ, Postnov DD, Lauritzen MJ. Modification of oxygen consumption and blood flow in mouse somatosensory cortex by cell-type-specific neuronal activity. *J Cereb Blood Flow Metab.* 2019; 271678X19882787.
 47. Anenberg E, Chan AW, Xie Y, LeDue JM, Murphy TH. Optogenetic stimulation of GABA neurons can decrease local neuronal activity while increasing cortical blood flow. *J Cereb Blood Flow Metab.* 2015;35: 1579–1586.
 48. Lee J, Stile CL, Bice AR, Rosenthal ZP, Yan P, Snyder AZ, et al. Opposed hemodynamic responses following increased excitation and parvalbumin-based inhibition. *J Cereb Blood Flow Metab.* 2020; 0271678X20930831.
 49. Logothetis NK. What we can do and what we cannot do with fMRI. *Nature.* 2008;453: 869–878.
 50. Marín O. Interneuron dysfunction in psychiatric disorders. *Nature Reviews Neuroscience.* 2012. pp. 107–120. doi:10.1038/nrn3155
 51. Palop JJ, Mucke L. Network abnormalities and interneuron dysfunction in Alzheimer disease. *Nat Rev Neurosci.* 2016;17: 777–792.
 52. Ferguson BR, Gao W-J. PV Interneurons: Critical Regulators of E/I Balance for Prefrontal Cortex-Dependent Behavior and Psychiatric Disorders. *Front Neural Circuits.* 2018;12: 37.
 53. Zhu Q, Naegele JR, Chung S. Cortical GABAergic Interneuron/Progenitor Transplantation as a Novel Therapy for Intractable Epilepsy. *Front Cell Neurosci.* 2018;12: 167.
 54. Dudek FE, Shao L-R. Loss of GABAergic Interneurons in Seizure-induced Epileptogenesis. *Epilepsy Curr.* 2003;3: 159–161.
 55. Lecrux C, Sandoe CH, Neupane S, Kropf P, Toussay X, Tong X-K, et al. Impact of Altered Cholinergic Tones on the Neurovascular Coupling Response to Whisker Stimulation. *J Neurosci.* 2017;37: 1518–1531.
 56. Lecrux C, Hamel E. Neuronal networks and mediators of cortical neurovascular coupling responses in normal and altered brain states. *Philos Trans R Soc Lond B Biol Sci.* 2016;371. doi:10.1098/rstb.2015.0350
 57. Perrenoud Q, Rossier J, Férézou I, Geoffroy H, Gallopin T, Vitalis T, et al. Activation of cortical 5-HT₃ receptor-expressing interneurons induces NO mediated vasodilatations and NPY mediated vasoconstrictions. *Front Neural Circuits.* 2012;6. doi:10.3389/fncir.2012.00050
 58. Zaldivar D, Rauch A, Whittingstall K, Logothetis NK, Goense J. Dopamine-induced dissociation of BOLD and neural activity in macaque visual cortex. *Curr Biol.* 2014;24: 2805–2811.

59. Zaldivar D, Rauch A, Logothetis NK, Goense J. Two distinct profiles of fMRI and neurophysiological activity elicited by acetylcholine in visual cortex. *Proc Natl Acad Sci U S A*. 2018;115: E12073–E12082.
60. Rauch A, Rainer G, Logothetis NK. The effect of a serotonin-induced dissociation between spiking and perisynaptic activity on BOLD functional MRI. *Proc Natl Acad Sci U S A*. 2008;105: 6759–6764.
61. Hock C, Villringer K, Müller-Spahn F, Wenzel R, Heekeren H, Schuh-Hofer S, et al. Decrease in parietal cerebral hemoglobin oxygenation during performance of a verbal fluency task in patients with Alzheimer’s disease monitored by means of near-infrared spectroscopy (NIRS) — correlation with simultaneous rCBF-PET measurements. *Brain Research*. 1997. pp. 293–303. doi:10.1016/s0006-8993(97)00122-4
62. Golby A, Silverberg G, Race E, Gabrieli S, O’Shea J, Knierim K, et al. Memory encoding in Alzheimer’s disease: an fMRI study of explicit and implicit memory. *Brain*. 2005;128: 773–787.
63. Rombouts SA, Barkhof F, Veltman DJ, Machielsen WC, Witter MP, Bierlaagh MA, et al. Functional MR imaging in Alzheimer’s disease during memory encoding. *AJNR Am J Neuroradiol*. 2000;21: 1869–1875.
64. Kato T, Knopman D, Liu H. Dissociation of regional activation in mild AD during visual encoding: a functional MRI study. *Neurology*. 2001;57: 812–816.
65. Hasselmo ME, Sarter M. Modes and models of forebrain cholinergic neuromodulation of cognition. *Neuropsychopharmacology*. 2011;36: 52–73.
66. Escartin C, Rouach N. Astroglial networking contributes to neurometabolic coupling. *Front Neuroenergetics*. 2013;5: 4.
67. Attwell D, Buchan AM, Charpak S, Lauritzen M, Macvicar BA, Newman EA. Glial and neuronal control of brain blood flow. *Nature*. 2010;468: 232–243.
68. Winship IR, Plaa N, Murphy TH. Rapid astrocyte calcium signals correlate with neuronal activity and onset of the hemodynamic response in vivo. *J Neurosci*. 2007;27: 6268–6272.
69. Biesecker KR, Srienc AI, Shimoda AM, Agarwal A, Bergles DE, Kofuji P, et al. Glial Cell Calcium Signaling Mediates Capillary Regulation of Blood Flow in the Retina. *J Neurosci*. 2016;36: 9435–9445.
70. Mishra A, Reynolds JP, Chen Y, Gourine AV, Rusakov DA, Attwell D. Astrocytes mediate neurovascular signaling to capillary pericytes but not to arterioles. *Nat Neurosci*. 2016;19: 1619–1627.
71. Schummers J, Yu H, Sur M. Tuned responses of astrocytes and their influence on hemodynamic signals in the visual cortex. *Science*. 2008;320: 1638–1643.
72. Zonta M, Angulo MC, Gobbo S, Rosengarten B, Hossmann K-A, Pozzan T, et al. Neuron-to-astrocyte signaling is central to the dynamic control of brain microcirculation. *Nature Neuroscience*. 2003. pp. 43–50. doi:10.1038/nn980
73. Takata N, Sugiura Y, Yoshida K, Koizumi M, Hiroshi N, Honda K, et al. Optogenetic

astrocyte activation evokes BOLD fMRI response with oxygen consumption without neuronal activity modulation. *Glia*. 2018;66: 2013–2023.

74. Nizar K, Uhlirova H, Tian P, Saisan PA, Cheng Q, Reznichenko L, et al. In vivo stimulus-induced vasodilation occurs without IP3 receptor activation and may precede astrocytic calcium increase. *J Neurosci*. 2013;33: 8411–8422.
75. Institoris Á, Rosenegger DG, Gordon GR. Arteriole dilation to synaptic activation that is sub-threshold to astrocyte endfoot Ca²⁺ transients. *J Cereb Blood Flow Metab*. 2015;35: 1411–1415.
76. Bonder DE, McCarthy KD. Astrocytic Gq-PCR-linked IP3R-dependent Ca²⁺ signaling does not mediate neurovascular coupling in mouse visual cortex in vivo. *J Neurosci*. 2014;34: 13139–13150.
77. Schulz K, Sydekum E, Krueppel R, Engelbrecht CJ, Schlegel F, Schröter A, et al. Simultaneous BOLD fMRI and fiber-optic calcium recording in rat neocortex. *Nat Methods*. 2012;9: 597–602.
78. Gu X, Chen W, Volkow ND, Koretsky AP, Du C, Pan Y. Synchronized Astrocytic Ca²⁺ Responses in Neurovascular Coupling during Somatosensory Stimulation and for the Resting State. *Cell Rep*. 2018;23: 3878–3890.
79. Kim KJ, Iddings JA, Stern JE, Blanco VM, Croom D, Kirov SA, et al. Astrocyte contributions to flow/pressure-evoked parenchymal arteriole vasoconstriction. *J Neurosci*. 2015;35: 8245–8257.
80. Mehina EMF, Murphy-Royal C, Gordon GR. Steady-State Free Ca²⁺ in Astrocytes Is Decreased by Experience and Impacts Arteriole Tone. *J Neurosci*. 2017;37: 8150–8165.
81. Di Castro MA, Chuquet J, Liaudet N, Bhaukaurally K, Santello M, Bouvier D, et al. Local Ca²⁺ detection and modulation of synaptic release by astrocytes. *Nat Neurosci*. 2011;14: 1276–1284.
82. Otsu Y, Couchman K, Lyons DG, Collot M, Agarwal A, Mallet J-M, et al. Calcium dynamics in astrocyte processes during neurovascular coupling. *Nat Neurosci*. 2015;18: 210–218.
83. Wang M, He Y, Sejnowski TJ, Yu X. Brain-state dependent astrocytic Ca²⁺ signals are coupled to both positive and negative BOLD-fMRI signals. *Proc Natl Acad Sci U S A*. 2018;115: E1647–E1656.
84. Stobart JL, Ferrari KD, Barrett MJP, Glück C, Stobart MJ, Zuend M, et al. Cortical Circuit Activity Evokes Rapid Astrocyte Calcium Signals on a Similar Timescale to Neurons. *Neuron*. 2018;98: 726–735.e4.
85. Lind BL, Brazhe AR, Jessen SB, Tan FCC, Lauritzen MJ. Rapid stimulus-evoked astrocyte Ca²⁺ elevations and hemodynamic responses in mouse somatosensory cortex in vivo. *Proc Natl Acad Sci U S A*. 2013;110: E4678–87.
86. Lind BL, Jessen SB, Lønstrup M, Joséphine C, Bonvento G, Lauritzen M. Fast Ca²⁺ responses in astrocyte end-feet and neurovascular coupling in mice. *Glia*. 2018;66: 348–358.

87. Uludag K, Müller-Bierl B, Ugurbil K. An integrative model for neuronal activity-induced signal changes for gradient and spin echo functional imaging. *NeuroImage*. 2009. p. S56. doi:10.1016/s1053-8119(09)70204-6
88. Ugurbil K. What is feasible with imaging human brain function and connectivity using functional magnetic resonance imaging. *Philos Trans R Soc Lond B Biol Sci*. 2016;371. doi:10.1098/rstb.2015.0361
89. Norris DG. Spin-echo fMRI: The poor relation? *Neuroimage*. 2012;62: 1109–1115.
90. Petzold GC, Murthy VN. Role of astrocytes in neurovascular coupling. *Neuron*. 2011;71: 782–797.
91. Iadecola C. The Neurovascular Unit Coming of Age: A Journey through Neurovascular Coupling in Health and Disease. *Neuron*. 2017;96: 17–42.
92. McConnell HL, Li Z, Woltjer RL, Mishra A. Astrocyte dysfunction and neurovascular impairment in neurological disorders: Correlation or causation? *Neurochem Int*. 2019;128: 70–84.
93. Pappas AC, Koide M, Wellman GC. Astrocyte Ca²⁺ Signaling Drives Inversion of Neurovascular Coupling after Subarachnoid Hemorrhage. *J Neurosci*. 2015;35: 13375–13384.
94. Cavaglia M, Dombrowski SM, Drazba J, VasANJI A, Bokesch PM, Janigro D. Regional variation in brain capillary density and vascular response to ischemia. *Brain Res*. 2001;910: 81–93.
95. Bohn KA, Adkins CE, Mittapalli RK, Terrell-Hall TB, Mohammad AS, Shah N, et al. Semi-automated rapid quantification of brain vessel density utilizing fluorescent microscopy. *J Neurosci Methods*. 2016;270: 124–131.
96. Hill RA, Tong L, Yuan P, Murikinati S, Gupta S, Grutzendler J. Regional Blood Flow in the Normal and Ischemic Brain Is Controlled by Arteriolar Smooth Muscle Cell Contractility and Not by Capillary Pericytes. *Neuron*. 2015;87: 95–110.
97. Attwell D, Mishra A, Hall CN, O'Farrell FM, Dalkara T. What is a pericyte? *J Cereb Blood Flow Metab*. 2016;36: 451–455.
98. Peppiatt CM, Howarth C, Mobbs P, Attwell D. Bidirectional control of CNS capillary diameter by pericytes. *Nature*. 2006;443: 700–704.
99. Hall CN, Reynell C, Gesslein B, Hamilton NB, Mishra A, Sutherland BA, et al. Capillary pericytes regulate cerebral blood flow in health and disease. *Nature*. 2014;508: 55–60.
100. Kisler K, Nelson AR, Rege SV, Ramanathan A, Wang Y, Ahuja A, et al. Pericyte degeneration leads to neurovascular uncoupling and limits oxygen supply to brain. *Nat Neurosci*. 2017;20: 406–416.
101. Grant RI, Hartmann DA, Underly RG, Berthiaume A-A, Bhat NR, Shih AY. Organizational hierarchy and structural diversity of microvascular pericytes in adult mouse cortex. *J Cereb Blood Flow Metab*. 2019;39: 411–425.
102. Rungta RL, Chaigneau E, Osmanski B-F, Charpak S. Vascular Compartmentalization of Functional Hyperemia from the Synapse to the Pia. *Neuron*. 2019;101: 762.

103. Longden TA, Dabertrand F, Koide M, Gonzales AL, Tykocki NR, Brayden JE, et al. Capillary K⁺-sensing initiates retrograde hyperpolarization to increase local cerebral blood flow. *Nat Neurosci.* 2017;20: 717–726.
104. Shaw K, Bell L, Boyd K, Grijseels DM, Clarke D. Hippocampus has lower oxygenation and weaker control of brain blood flow than cortex, due to microvascular differences. *bioRxiv.* 2019. Available: <https://www.biorxiv.org/content/10.1101/835728v1.abstract>
105. Nelson AR, Sagare MA, Wang Y, Kisler K, Zhao Z, Zlokovic BV. Channelrhodopsin Excitation Contracts Brain Pericytes and Reduces Blood Flow in the Aging Mouse Brain in vivo. *Front Aging Neurosci.* 2020;12: 108.
106. Tieu T, McDowell K, Faino A, Kelly A, Shih AY. Brain capillary pericytes exert a substantial but slow influence on blood flow. *bioRxiv.* 2020. Available: <https://www.biorxiv.org/content/10.1101/2020.03.26.008763v1.abstract>
107. Lee J, Wu W, Boas DA. Early capillary flux homogenization in response to neural activation. *J Cereb Blood Flow Metab.* 2016;36: 375–380.
108. Schulte ML, Wood JD, Hudetz AG. Cortical electrical stimulation alters erythrocyte perfusion pattern in the cerebral capillary network of the rat. *Brain Res.* 2003;963: 81–92.
109. Rasmussen PM, Jespersen SN, Østergaard L. The effects of transit time heterogeneity on brain oxygenation during rest and functional activation. *J Cereb Blood Flow Metab.* 2015;35: 432–442.
110. Li B, Esipova TV, Sencan I, Kiliç K, Fu B, Desjardins M, et al. More homogeneous capillary flow and oxygenation in deeper cortical layers correlate with increased oxygen extraction. *Elife.* 2019;8. doi:10.7554/eLife.42299
111. Blinder P, Tsai PS, Kaufhold JP, Knutsen PM, Suhl H, Kleinfeld D. The cortical angiome: an interconnected vascular network with noncolumnar patterns of blood flow. *Nat Neurosci.* 2013;16: 889–897.
112. Cai C, Fordsmann JC, Jensen SH, Gesslein B, Lønstrup M, Hald BO, et al. Stimulation-induced increases in cerebral blood flow and local capillary vasoconstriction depend on conducted vascular responses. *Proc Natl Acad Sci U S A.* 2018;115: E5796–E5804.
113. Tian P, Teng IC, May LD, Kurz R, Lu K, Scadeng M, et al. Cortical depth-specific microvascular dilation underlies laminar differences in blood oxygenation level-dependent functional MRI signal. *Proc Natl Acad Sci U S A.* 2010;107: 15246–15251.
114. Kornfield TE, Newman EA. Regulation of blood flow in the retinal trilaminar vascular network. *J Neurosci.* 2014;34: 11504–11513.
115. Nortley R, Korte N, Izquierdo P, Hirunpattarasilp C, Mishra A, Jaunmuktane Z, et al. Amyloid β oligomers constrict human capillaries in Alzheimer's disease via signaling to pericytes. *Science.* 2019;365. doi:10.1126/science.aav9518
116. Dietrich HH, Xiang C, Han BH, Zipfel GJ, Holtzman DM. Soluble amyloid- β , effect on

- cerebral arteriolar regulation and vascular cells. *Mol Neurodegener.* 2010;5: 15.
117. Niwa K, Porter VA, Kazama K, Cornfield D, Carlson GA, Iadecola C. A β -peptides enhance vasoconstriction in cerebral circulation. *American Journal of Physiology-Heart and Circulatory Physiology.* 2001. pp. H2417–H2424.
doi:10.1152/ajpheart.2001.281.6.h2417
 118. Han BH, Zhou M-L, Abousaleh F, Brendza RP, Dietrich HH, Koenigsnecht-Talboo J, et al. Cerebrovascular dysfunction in amyloid precursor protein transgenic mice: contribution of soluble and insoluble amyloid-beta peptide, partial restoration via gamma-secretase inhibition. *J Neurosci.* 2008;28: 13542–13550.
 119. Kimbrough IF, Robel S, Roberson ED, Sontheimer H. Vascular amyloidosis impairs the gliovascular unit in a mouse model of Alzheimer's disease. *Brain.* 2015;138: 3716–3733.
 120. Segal SS. Integration and Modulation of Intercellular Signaling Underlying Blood Flow Control. *J Vasc Res.* 2015;52: 136–157.
 121. Beach JM, McGahren ED, Duling BR. Capillaries and arterioles are electrically coupled in hamster cheek pouch. *Am J Physiol.* 1998;275: H1489–96.
 122. Oku H, Kodama T, Sakagami K, Puro DG. Diabetes-induced disruption of gap junction pathways within the retinal microvasculature. *Invest Ophthalmol Vis Sci.* 2001;42: 1915–1920.
 123. Iadecola C, Yang G, Ebner TJ, Chen G. Local and propagated vascular responses evoked by focal synaptic activity in cerebellar cortex. *J Neurophysiol.* 1997;78: 651–659.
 124. Guerra G, Lucariello A, Perna A, Botta L, De Luca A, Moccia F. The Role of Endothelial Ca²⁺ Signaling in Neurovascular Coupling: A View from the Lumen. *Int J Mol Sci.* 2018;19. doi:10.3390/ijms19040938
 125. Rosenblum WI. Endothelium-dependent responses in the microcirculation observed in vivo. *Acta Physiol.* 2018;224: e13111.
 126. Zechariah A, Tran CHT, Hald BO, Sandow SL, Sancho M, Kim MSM, et al. Intercellular Conduction Optimizes Arterial Network Function and Conserves Blood Flow Homeostasis During Cerebrovascular Challenges. *Arterioscler Thromb Vasc Biol.* 2020;40: 733–750.
 127. Kovacs-Oller T, Ivanova E, Bianchimano P, Sagdullaev BT. The pericyte connectome: spatial precision of neurovascular coupling is driven by selective connectivity maps of pericytes and endothelial cells and is disrupted in diabetes. *Cell Discovery.* 2020. doi:10.1038/s41421-020-0180-0
 128. Stobart JLL, Lu L, Anderson HDI, Mori H, Anderson CM. Astrocyte-induced cortical vasodilation is mediated by D-serine and endothelial nitric oxide synthase. *Proc Natl Acad Sci U S A.* 2013;110: 3149–3154.
 129. Hogan-Cann AD, Lu P, Anderson CM. Endothelial NMDA receptors mediate activity-dependent brain hemodynamic responses in mice. *Proc Natl Acad Sci U S A.* 2019;116: 10229–10231.

130. Chen BR, Kozberg MG, Bouchard MB, Shaik MA, Hillman EMC. A critical role for the vascular endothelium in functional neurovascular coupling in the brain. *J Am Heart Assoc.* 2014;3: e000787.
131. O'Herron P, Chhatbar PY, Levy M, Shen Z, Schramm AE, Lu Z, et al. Neural correlates of single-vessel haemodynamic responses in vivo. *Nature.* 2016. pp. 378–382. doi:10.1038/nature17965
132. Jukovskaya N, Tiret P, Lecoq J, Charpak S. What Does Local Functional Hyperemia Tell about Local Neuronal Activation? *Journal of Neuroscience.* 2011. pp. 1579–1582. doi:10.1523/jneurosci.3146-10.2011
133. Sheth SA, Nemoto M, Guiou M, Walker M, Pouratian N, Hageman N, et al. Columnar specificity of microvascular oxygenation and volume responses: implications for functional brain mapping. *J Neurosci.* 2004;24: 634–641.
134. Frostig RD, Lieke EE, Ts'o DY, Grinvald A. Cortical functional architecture and local coupling between neuronal activity and the microcirculation revealed by in vivo high-resolution optical imaging of intrinsic signals. *Proc Natl Acad Sci U S A.* 1990;87: 6082–6086.
135. Malonek D, Grinvald A. Interactions between electrical activity and cortical microcirculation revealed by imaging spectroscopy: implications for functional brain mapping. *Science.* 1996;272: 551–554.
136. Hu X, Yacoub E. The story of the initial dip in fMRI. *NeuroImage.* 2012. pp. 1103–1108. doi:10.1016/j.neuroimage.2012.03.005
137. Menon RS, Ogawa S, Hu X, Strupp JP, Anderson P, Uğurbil K. BOLD based functional MRI at 4 Tesla includes a capillary bed contribution: echo-planar imaging correlates with previous optical imaging using intrinsic signals. *Magn Reson Med.* 1995;33: 453–459.
138. Kim DS, Duong TQ, Kim SG. High-resolution mapping of iso-orientation columns by fMRI. *Nat Neurosci.* 2000;3: 164–169.
139. Zhang T, Wu DM, Xu G-Z, Puro DG. The electrotonic architecture of the retinal microvasculature: modulation by angiotensin II. *J Physiol.* 2011;589: 2383–2399.
140. Chow BW, Nuñez V, Kaplan L, Granger AJ, Bistrong K, Zucker HL, et al. Caveolae in CNS arterioles mediate neurovascular coupling. *Nature.* 2020;579: 106–110.
141. Harraz OF, Longden TA, Hill-Eubanks D, Nelson MT. PIP2 depletion promotes TRPV4 channel activity in mouse brain capillary endothelial cells. *Elife.* 2018;7. doi:10.7554/eLife.38689
142. Ivanova E, Kovacs-Oller T, Sagdullaev BT. Vascular Pericyte Impairment and Connexin43 Gap Junction Deficit Contribute to Vasomotor Decline in Diabetic Retinopathy. *J Neurosci.* 2017;37: 7580–7594.
143. Byrd JB, Ram CVS, Lerma EV. Pharmacologic treatment of hypertension. *Nephrology Secrets.* 2019. pp. 477–482. doi:10.1016/b978-0-323-47871-7.00078-2
144. Blockley NP, Griffeth VEM, Buxton RB. A general analysis of calibrated BOLD

methodology for measuring CMRO₂ responses: comparison of a new approach with existing methods. *Neuroimage*. 2012;60: 279–289.

145. Alle H, Roth A, Geiger JRP. Energy-efficient action potentials in hippocampal mossy fibers. *Science*. 2009;325: 1405–1408.
146. Carter BC, Bean BP. Sodium entry during action potentials of mammalian neurons: incomplete inactivation and reduced metabolic efficiency in fast-spiking neurons. *Neuron*. 2009;64: 898–909.
147. Yu Y, Herman P, Rothman DL, Agarwal D, Hyder F. Evaluating the gray and white matter energy budgets of human brain function. *J Cereb Blood Flow Metab*. 2018;38: 1339–1353.
148. Mercer RW, Dunham PB. Membrane-bound ATP fuels the Na/K pump. Studies on membrane-bound glycolytic enzymes on inside-out vesicles from human red cell membranes. *J Gen Physiol*. 1981;78: 547–568.
149. Masamoto K, Vazquez A, Wang P, Kim S-G. Trial-by-trial relationship between neural activity, oxygen consumption, and blood flow responses. *Neuroimage*. 2008;40: 442–450.
150. Mathiesen C, Caesar K, Thomsen K, Hoogland TM, Witgen BM, Brazhe A, et al. Activity-dependent increases in local oxygen consumption correlate with postsynaptic currents in the mouse cerebellum in vivo. *J Neurosci*. 2011;31: 18327–18337.
151. Abeles M. *Corticonics: Neural Circuits of the Cerebral Cortex*. Cambridge University Press; 1991.
152. Villa KL, Nedivi E. Excitatory and Inhibitory Synaptic Placement and Functional Implications. In: Emoto K, Wong R, Huang E, Hoogenraad C, editors. *Dendrites: Development and Disease*. Tokyo: Springer Japan; 2016. pp. 467–487.
153. McCasland JS, Hibbard LS. GABAergic neurons in barrel cortex show strong, whisker-dependent metabolic activation during normal behavior. *J Neurosci*. 1997;17: 5509–5527.
154. Buzsáki G, Kaila K, Raichle M. Inhibition and brain work. *Neuron*. 2007;56: 771–783.
155. Gan J, Weng S-M, Pernía-Andrade AJ, Csicsvari J, Jonas P. Phase-Locked Inhibition, but Not Excitation, Underlies Hippocampal Ripple Oscillations in Awake Mice In Vivo. *Neuron*. 2017;93: 308–314.
156. English DF, Peyrache A, Stark E, Roux L, Vallentin D, Long MA, et al. Excitation and inhibition compete to control spiking during hippocampal ripples: intracellular study in behaving mice. *J Neurosci*. 2014;34: 16509–16517.
157. Royzen F, Williams S, Fernandez FR, White JA. Balanced synaptic currents underlie low-frequency oscillations in the subiculum. *Hippocampus*. 2019;29: 1178–1189.
158. Haider B, Duque A, Hasenstaub AR, McCormick DA. Neocortical network activity in vivo is generated through a dynamic balance of excitation and inhibition. *J Neurosci*. 2006;26: 4535–4545.
159. Denève S, Machens CK. Efficient codes and balanced networks. *Nat Neurosci*.

- 2016;19: 375–382.
160. Bhatia A, Moza S, Bhalla US. Precise excitation-inhibition balance controls gain and timing in the hippocampus. *Elife*. 2019;8. doi:10.7554/eLife.43415
 161. Betterton RT, Broad LM, Tsaneva-Atanasova K, Mellor JR. Acetylcholine modulates gamma frequency oscillations in the hippocampus by activation of muscarinic M1 receptors. *Eur J Neurosci*. 2017;45: 1570–1585.
 162. Garcia-Junco-Clemente P, Tring E, Ringach DL, Trachtenberg JT. State-Dependent Subnetworks of Parvalbumin-Expressing Interneurons in Neocortex. *Cell Rep*. 2019;26: 2282–2288.e3.
 163. Lee S, Hjerling-Leffler J, Zagha E, Fishell G, Rudy B. The largest group of superficial neocortical GABAergic interneurons expresses ionotropic serotonin receptors. *J Neurosci*. 2010;30: 16796–16808.
 164. Kann O. The interneuron energy hypothesis: Implications for brain disease. *Neurobiol Dis*. 2016;90: 75–85.
 165. Gulyás AI, Buzsáki G, Freund TF, Hirase H. Populations of hippocampal inhibitory neurons express different levels of cytochrome c. *Eur J Neurosci*. 2006;23: 2581–2594.
 166. Hu H, Jonas P. A supercritical density of Na(+) channels ensures fast signaling in GABAergic interneuron axons. *Nat Neurosci*. 2014;17: 686–693.
 167. Vazquez AL, Fukuda M, Kim S-G. Inhibitory Neuron Activity Contributions to Hemodynamic Responses and Metabolic Load Examined Using an Inhibitory Optogenetic Mouse Model. *Cereb Cortex*. 2018;28: 4105–4119.
 168. Freund TF, Buzsáki G. Interneurons of the hippocampus. *Hippocampus*. 1996;6: 347–470.
 169. Valtschanoff JG, Weinberg RJ, Kharazia VN, Schmidt HH, Nakane M, Rustioni A. Neurons in rat cerebral cortex that synthesize nitric oxide: NADPH diaphorase histochemistry, NOS immunocytochemistry, and colocalization with GABA. *Neurosci Lett*. 1993;157: 157–161.
 170. Ackermann RF, Finch DM, Babb TL, Engel J Jr. Increased glucose metabolism during long-duration recurrent inhibition of hippocampal pyramidal cells. *J Neurosci*. 1984;4: 251–264.
 171. Angenstein F. The role of ongoing neuronal activity for baseline and stimulus-induced BOLD signals in the rat hippocampus. *NeuroImage*. 2019. p. 116082. doi:10.1016/j.neuroimage.2019.116082
 172. Pellerin L, Magistretti PJ. Glial Energy Metabolism: Overview. *Encyclopedia of Neuroscience*. 2009. pp. 783–788. doi:10.1016/b978-008045046-9.01708-3
 173. Macaisa CM, Watabe T, Liu Y, Romanov V, Kanai Y, Horitsugi G, et al. Preserved Cerebral Oxygen Metabolism in Astrocytic Dysfunction: A Combination Study of 15O-Gas PET with 14C-Acetate Autoradiography. *Brain Sci*. 2019;9. doi:10.3390/brainsci9050101
 174. Fernández-Moncada I, Ruminot I, Robles-Maldonado D, Alegría K, Deitmer JW,

- Barros LF. Neuronal control of astrocytic respiration through a variant of the Crabtree effect. *Proc Natl Acad Sci U S A*. 2018;115: 1623–1628.
175. Nortley R, Attwell D. Control of brain energy supply by astrocytes. *Curr Opin Neurobiol*. 2017;47: 80–85.
176. Kasischke KA, Vishwasrao HD, Fisher PJ, Zipfel WR, Webb WW. Neural activity triggers neuronal oxidative metabolism followed by astrocytic glycolysis. *Science*. 2004;305: 99–103.
177. Rao VTS, Khan D, Cui Q-L, Fuh S-C, Hossain S, Almazan G, et al. Distinct age and differentiation-state dependent metabolic profiles of oligodendrocytes under optimal and stress conditions. *PLoS One*. 2017;12: e0182372.
178. Harris JJ, Attwell D. The energetics of CNS white matter. *J Neurosci*. 2012;32: 356–371.
179. Tsai AG, Friesenecker B, Mazzoni MC, Kerger H, Buerk DG, Johnson PC, et al. Microvascular and tissue oxygen gradients in the rat mesentery. *Proc Natl Acad Sci U S A*. 1998;95: 6590–6595.
180. Duling BR, Kuschinsky W, Wahl M. Measurements of the perivascular PO₂ in the vicinity of the pial vessels of the cat. *Pflügers Archiv European Journal of Physiology*. 1979. pp. 29–34. doi:10.1007/bf00584471
181. Buerk DG, Goldstick TK. Arterial wall oxygen consumption rate varies spatially. *Am J Physiol*. 1982;243: H948–58.
182. Gould IG, Tsai P, Kleinfeld D, Linninger A. The capillary bed offers the largest hemodynamic resistance to the cortical blood supply. *J Cereb Blood Flow Metab*. 2017;37: 52–68.
183. Huchzermeyer C, Berndt N, Holzhütter H-G, Kann O. Oxygen consumption rates during three different neuronal activity states in the hippocampal CA3 network. *J Cereb Blood Flow Metab*. 2013;33: 263–271.
184. Schmid F, Barrett MJP, Jenny P, Weber B. Vascular density and distribution in neocortex. *Neuroimage*. 2019;197: 792–805.